Linking Hadley circulation and storm tracks in a conceptual model of the atmospheric energy balance

Cheikh Mbengue[1] * and Tapio Schneider[2]

[1] *University of Oxford, Oxford, United Kingdom*

[2] *California Institute of Technology, California, United States of America*

* *Corresponding author address:* Cheikh Mbengue, Atmospheric, Oceanic, and Planetary Physics, Sherrington Road, Oxford OX1 3PU, United Kingdom.

E-mail: c.mbengue@wolfson.oxon.org

ABSTRACT

Midlatitude storm tracks shift in response to climate change and natural climate variations such as El Niño, but the dynamical mechanisms controlling these shifts are not well established. This paper develops an energy balance model that shows how shifts of the Hadley cell terminus and changes of the meridional energy flux out of the Hadley cell can drive shifts of storm tracks, identified as extrema of the atmospheric meridional eddy energy flux. The distance between the Hadley cell terminus and the storm tracks is primarily controlled by the energy flux out of the Hadley cell. Because tropical forcings alone can modify the Hadley cell terminus, they can also shift extratropical storm tracks, as demonstrated through simulations with an idealized GCM. Additionally, a strengthening of the meridional temperature gradient at the terminus and hence of the energy flux out of the Hadley cell can reduce the distance between the Hadley cell terminus and the storm tracks, enabling storm-track shifts that do not parallel shifts of the Hadley cell terminus. Thus, with the aid of the energy balance model and supporting GCM simulations, a closed theory of storm-track shifts emerges.

1. Introduction

Midlatitude storm tracks are important components of Earth's general circulation. They redistribute large amounts of energy, moisture, and angular momentum within the atmosphere, and so determine weather and climate patterns over Earth's surface. Storm tracks have been characterized in several ways in the literature (Chang et al. 2002). A common method uses eddy fields bandpass-filtered to synoptic time scales and identifies storm tracks as regions of large eddy amplitudes (Blackmon 1976; Blackmon et al. 1977; Hoskins and Valdes 1990). It is also possible to use statistics obtained from tracking individual cyclones and anticyclones (Murray and Simmonds 1991; Hoskins and Hodges 2002). Generally, although not always, such different ways of identifying storm tracks agree broadly, in the identification of both, storm tracks in the present climate and their changes in different climates.

It has been extensively described how the structure, strength, and location of midlatitude storm tracks changes as the climate changes (Geng and Sugi 2003; Yin 2005; Bengtsson et al. 2006; Ulbrich et al. 2008; O'Gorman 2010; Barnes and Polvani 2013; Chang 2013; Simpson et al. 2014). These changes affect precipitation and severe weather patterns across midlatitudes. Thus, it is important to understand the mechanisms controlling the storm-track response to perturbations in climate. Although several theories of storm-track shifts have been suggested (Kushner and Polvani 2004; Yin 2005; Chen and Held 2007; Lorenz and DeWeaver 2007; Chen et al. 2008; Lu et al. 2010; Butler et al. 2010; Kidston et al. 2010; Riviere 2011; Butler et al. 2011; Lorenz 2014), a generally accepted one remains elusive because dynamical actors feed back onto each other or act in compensating ways. A closed theory linking them remains outstanding.

To understand the mechanisms of storm-track shifts, in a previous study we used a dry idealized general circulation model (GCM) to link shifts in midlatitude storm tracks to shifts in near-surface midlatitude temperature gradients (Mbengue and Schneider 2013, 2017; hereafter MS13 and MS17). We observed that the Hadley cell terminus often shifts

in tandem with the storm tracks, as also seen by Kang and Polvani (2011) and Ceppi and Hartmann (2013). It is possible that the two influence each other, but the causal link between them had remained unclear. Some studies suggest that extratropical dynamics lead to changes in the extent of the Hadley cell. For example, Chen and Held (2007) posit that changes in the eastward phase speed of extratropical eddies modify the subtropical wave-breaking latitude, where eddy angular momentum fluxes diverge, and as a result modify the Hadley cell terminus, considered to be the latitude where the eddy angular momentum flux divergence changes sign (Korty and Schneider 2008). Alternatively, the extent of the Hadley cell may be controlled by measures of baroclinicity, such as the subtropical static stability and meridional temperature gradients, and may change as these change (Walker and Schneider 2006; Frierson et al. 2007b; Lu et al. 2007; Korty and Schneider 2008; O'Gorman 2011; Mbengue and Schneider 2013; Levine and Schneider 2015). The same baroclinicity measures also affect the storm track position, but this view leaves unclear how storm tracks and the Hadley cell terminus are dynamically linked.

The idea that shifts in the Hadley cell terminus could cause shifts in storm tracks was conjecture until numerical experiments by Schneider (2004) and MS13 showed that storm tracks shift poleward in response to increases in convective static stability in the deep tropics alone (within $\pm 10^\circ$ latitude). The forcing, unable to affect extratropical eddies directly, needs a tropical mechanism by which it can be translated into a poleward shift of midlatitude storm tracks. The tandem shifts of the Hadley terminus with the storm tracks make the Hadley circulation a candidate for communicating the changes in tropical convective static stability to the extratropics. MS17 linked shifts in midlatitude storm tracks, identified as eddy kinetic energy maxima, to shifts in maxima of near-surface meridional temperature gradients (or of baroclinic mean available potential energy more generally). Because meridional eddy energy fluxes in midlatitudes have a diffusive character (Kushner and Held 1998; Held 1999), maxima of near-surface meridional temperature gradients approximately coincide with maxima of meridional eddy energy fluxes, which have also been used to identify storm tracks (e.g.,

Schneider and Walker 2006, 2008). Therefore, it remains to link shifts in the Hadley cell terminus to shifts in near-surface meridional temperature gradients or eddy energy fluxes. Doing so would yield a closed theory for storm-track shifts, at least in dry atmospheres.

In this paper, we develop a zonal-mean energy balance model (EBM, see North et al. (1981) for a review) that links Hadley cell changes to extratropical temperature gradients and meridional energy fluxes. EBMs have a long history, and important insights have been derived from them (Budyko 1969; Sellers 1969; Held and Suarez 1974; North 1975a,b; Lindzen and Farrell 1981; Flannery 1984; Roe and Lindzen 2001; Frierson et al. 2007a). While they have primarily focused on energy transport by extratropical eddies, Hadley circulation dynamics have also been incorporated in some EBMs (e.g., Lindzen and Farrell 1981). What is new about the EBM used here is that it models energy transport by the Hadley cell and extratropical eddies explicitly and interactively through diffusive closures, with an enhanced diffusivity within the Hadley cell to represent its strong energy transport. We link shifts in the Hadley cell energy transport to shifts in near-surface temperature gradients, energy fluxes, and, by extension, to storm-track shifts.

Because the tropical Hadley cell is controlled by complex and generally not diffusive dynamics (e.g., Schneider and Walker 2006; Schneider et al. 2010) and extratropical eddy energy transport has contributions from non-local latent energy transport (Pierrehumbert 2002; Pierrehumbert et al. 2007; O'Gorman and Schneider 2006, 2008), local diffusive parameterizations of meridional turbulent energy transport may seem questionable at first glance. Nonetheless, diffusive parameterizations of meridional energy transport are used widely in EBMs (e.g., Sellers 1969; Held and Suarez 1974; North 1975a,b; Frierson et al. 2007a). One reason is their mathematical expedience. Additionally, there is a weak separation of the $O(1000$ km) scales of Lagrangian air parcel displacements and the planetary scales over which near-surface temperature varies meridionally, providing some justification for diffusive eddy closures in the extratropics, at least for dry static energy fluxes (e.g., Corrsin 1974; Held 1999; Schneider et al. 2015). Empirically, diffusive closures have also been found to

work well on sufficiently long timescales in the extratropics, even for moist static energy fluxes (Lorenz 1979; Kushner and Held 1998; Frierson et al. 2007a; Roe et al. 2015). In the tropics, the primary function of the parameterized energy flux in our model is to strongly reduce meridional temperature gradients (Charney 1963; Sobel et al. 2001), and the precise form of the transport turns out to be unimportant for our results.

Section 2 gives a brief description of the idealized GCM that motivates and supports our investigations. Section 3 presents the diffusive EBM and the Hadley circulation parametrization. This is followed by an analysis of solutions of the EBM and idealized dry GCM simulations in Section 3. Section 4 synthesizes and discusses the implications of this work.

2. Idealized GCM

The GCM uses the dry dynamical core of the GFDL's Flexible Modeling System to solve the primitive equations on a sphere using a spectral transform method at T85 horizontal resolution, with 30 unevenly-spaced sigma levels. The GCM is the same one used in MS13 and MS17; it is described in detail in Schneider (2004) and Schneider and Walker (2006). The model is forced using Newtonian relaxation towards a statically unstable radiative-equilibrium profile on a timescale of 7 days near the surface and 50 days away from the surface. Standard Earth values are used for physical parameters within the model. The model has no continents, and no explicit representation of moisture or latent heat release in phase changes of water.

In the GCM, convection is parameterized using a quasi-equilibrium scheme that relaxes temperatures in an atmospheric column towards a prescribed lapse rate $\gamma\Gamma_d$ whenever the column is convectively less stable. Here, $0 < \gamma \leq 1$ is a rescaling parameter and Γ_d is the dry adiabatic lapse rate. Increasing γ increases the convective lapse rate and reduces the static stability of the temperature profile to which the convection schemes relaxes atmospheric columns. A rescaling parameter $\gamma < 1$ mimics some of the effects of latent heat release

in moist convection, in that it leads to convective temperature profiles that are statically more stable than a dry adiabat. In MS13 and MS17, we varied the rescaling parameter γ separately near the equator (γ_e, at latitude $|\phi| < 10^\circ$) and in the rest of the atmosphere (γ_x) to investigate the effect of deep-tropical static stability changes on extratropical storm tracks.

3. Diffusive EBM

We construct a zonal-mean EBM using the elements we deem important for understanding the mechanisms of storm-track shifts seen in dry atmospheres. Temperature in the EBM represents near-surface temperatures just above the boundary layer because diffusive eddy-transport closures have been found to apply best near the surface (Kushner and Held 1998; Held 1999). The midlatitude storm-track latitude is identified as the latitude of maximum absolute value of meridional temperature gradients, which was found to be a good indicator of storm-track latitude in the dry GCM simulations (MS17). With diffusive eddy flux closures, the latitude of maximal meridional temperature gradients corresponds to the latitude of maximum meridional eddy energy flux, or approximately (up to cosine factors), the latitude of zero meridional eddy energy flux divergence. The storm-track problem is distilled to a question of the interactive relationship among near-surface meridional temperature gradients, Hadley circulation dynamics, and meridional eddy energy transport.

Our EBM lacks several processes postulated to be important for storm-track shifts. For example, there is no explicit representation of eddy phase speed feedbacks, nor are the effects of changes in extratropical static stability represented. Moreover, the model does not consider the vertical structure of the atmosphere beyond static stability effects that are included in the Hadley cell parameterization. The principal advantage of the EBM is its simplicity. Any storm-track shifts within this EBM stand a better chance of being mechanistically explainable. Additional processes not considered here (e.g., energy transport

by stationary eddies) may be added later, or their effect on storm tracks can be inferred to the extent they can be taken as independent of transient eddies.

The diffusive EBM equation in spherical coordinates can be written as

$$\partial_t T(\phi) = \frac{\partial_\phi \left[D(\phi, \phi_h) \cos\phi \partial_\phi \right] T(\phi)}{R^2 \cos\phi} - \frac{T(\phi) - E(\phi)}{\tau_{\text{rad}}}, \tag{1}$$

with polar boundary condition

$$\partial_\phi T(-\pi/2) = \partial_\phi T(\pi/2) = 0. \tag{2}$$

Here, T is temperature, ϕ is latitude, $D(\phi, \phi_h)$ is the diffusivity, which may be latitude dependent and also depends on the Hadley cell terminus at latitude ϕ_h; R is the radius of the Earth; $E(\phi)$ is the radiative-equilibrium temperature profile; and τ_{rad} is a radiative relaxation timescale. This radiative forcing is similar to that in the GCM in MS13 and MS17.

The energy balance (1) states that the evolution of temperature (or energy) in a given latitude band (left-hand side) is balanced by the energy flux into that latitude band (first term on the right) and by the net diabatic heating or cooling in the latitude band (second term on the right). Meridional energy fluxes at the poles are zero (2). The forcing and flux terms are specified as follows.

a. Radiative forcing

Shortwave heating, long-wave cooling, and sensible and latent surface energy fluxes are parametrized using linear relaxation toward a prescribed radiative-equilibrium temperature profile $E(\phi)$ over a fixed radiative timescale τ_{rad}. The radiative-equilibrium profile $E(\phi)$ is the same as in the idealized dry GCM and mimics annual-mean conditions on Earth,

$$E(\phi) = \bar{T}_E + \Delta_H (1/3 - \sin^2\phi). \tag{3}$$

Here, $\bar{T}_E$ is the global-mean temperature and Δ_H is the pole-equator temperature contrast in radiative equilibrium.

b. Eddy energy transport

The meridional temperature (energy) flux can be decomposed as

$$[\overline{vT}] = [\overline{v}][\overline{T}] + [\overline{v'T'}] + [\overline{v}^*\ \overline{T}^*], \tag{4}$$

where the first term on the right-hand side is the meridional energy flux owing to mean circulations, the second term is the transient eddy energy flux, and the third is the stationary eddy energy flux (see Peixoto and Oort 1992). The overbar represents a temporal mean, and primes departures therefrom. The square brackets represent a zonal mean along a latitude circle, and asterisks departures therefrom. The GCM we have used in the previous studies, which we also refer to throughout this paper, has no means to excite stationary zonal asymmetries; hence, we ignore the last term on the right-hand side for now. Thus, a parameterization for the meridional energy transport requires finding a relationship for the flux $[\overline{vT}] = [\bar{v}][\bar{T}] + [\overline{v'T'}]$.

Transient eddy energy transport is modeled diffusively. We assume that the diffusive fluxes are proportional to the mean meridional temperature gradient, so that the meridional flux divergence in spherical coordinates becomes

$$\mathrm{div}[\overline{v'T'}] = -\frac{\partial_\phi \left[D(\phi, \phi_h)\cos(\phi)\partial_\phi\right] T}{R^2\cos(\phi)}. \tag{5}$$

In the extratropics ($|\phi| > \phi_h$), we use a constant diffusivity, $D(\phi, \phi_h) = D_x$, obtained from the empirical mean near-surface eddy diffusivity in the GCM simulations. Since transient eddies dominate the energy transport in the extratropics and have a fairly barotropic structure (Peixoto and Oort 1992; Schneider and Walker 2008), this is an adequate representation of the total transport in the extratropics (Held 1999).

Figure 1 shows the near-surface eddy diffusivity $D = -\{\overline{v'\theta'}\}/\{\partial_y\theta\}$ computed from the GCM. Here, the curly bracket means a near-surface vertical average between $\sigma = 0.8$ and $\sigma = 1.0$. Figure 1a shows the eddy diffusivity in simulations in which the mean radiative-equilibrium temperature is varied, with an Earth-like convective lapse rate ($\gamma_e = 0.7$) in

the deep tropics and a dry adiabatic convective lapse rate ($\gamma_x = 1$) in the extratropics. Figure 1b shows the eddy diffusivity response to changes solely in deep-tropical convective stability (γ_e), while temperatures outside the deep tropics continue to be relaxed toward a dry adiabat ($\gamma_x = 1$). In both sets of simulations, the strongest variations in diffusivity with latitude occur in the subtropics. In the simulations varying mean temperatures, the diffusivity varies with climate outside the Hadley cell terminus. In contrast, in simulations varying deep-tropical convective stability, the diffusivity is relatively constant with climate outside the Hadley terminus. While approximating the eddy diffusivity D_x through a constant in the EBM is not quantitatively accurate, Fig. 1 shows that this may be a useful first approximation for purposes of understanding how the storm track position relates to the atmospheric energy balance.

The variations of diffusivity with latitude and climate in Fig. 1 suggest that a more accurate representation would result from using a diffusivity that depends on latitude and climate. The maximum near-surface eddy diffusivity in the GCM simulations occurs just poleward of the Hadley cell terminus, implying enhanced eddy transport there. There is a modest poleward shift in the maximum of the near-surface eddy diffusivity with increasing mean radiative-equilibrium temperature, and a significant poleward shift with increasing deep-tropical convective stability. The eddy diffusivity's magnitude also increases as the mean radiative-equilibrium temperature or the convective stability increases. These changes in diffusivity suggest that eddy length and/or velocity scales have changed (Swanson and Pierrehumbert 1997; Held 1999). One may try to capture them by using a diffusive parameterization that is a function of the meridional temperature or potential temperature gradient, $\partial_y \bar{\theta}$. Eddy potential temperature fluxes in dry GCM simulations generally scale with a function of static stability and MAPE, which in strongly baroclinic regimes imply an approximate $\left(\partial_y \bar{\theta}\right)^{3/2}$ dependence of the fluxes (Schneider and Walker 2008). This would suggest a diffusivity that depends like $\left(\partial_y \bar{\theta}\right)^{1/2}$ on potential temperature gradients. However, this dependence is weak, and so we neglect it here. It will turn out that the EBM captures

essential features of the storm track shifts seen in the GCM with a constant extratropical diffusivity.

c. *Hadley cell energy transport*

In the tropics ($|\phi| < \phi_h$), transport by the mean meridional circulation must also be considered. To represent it, we use an enhanced diffusivity D_t at latitudes $|\phi| < \phi_h$. This enhanced diffusivity represents the fact that in the tropics, near the top of the planetary boundary layer, temperature gradients are rather weak because of efficient redistribution of energy (Charney 1963; Schneider 1977; Schneider and Lindzen 1977; Lindzen and Farrell 1977; Held and Hou 1980; Sobel et al. 2001).

The total diffusivity in the EBM thus takes the form

$$D(\phi, \phi_h) = D_x + (D_t - D_x)\mathcal{S}(\phi, \phi_h), \tag{6}$$

where $\mathcal{S}(\phi, \phi_h)$ is a smoothed top-hat function,

$$\mathcal{S}(\phi, \phi_h) = \frac{1}{2}\left[1 - \tanh\left(\pi\frac{\phi - \phi_h}{\phi_h}\right)\tanh\left(\pi\frac{\phi + \phi_h}{\phi_h}\right)\right], \tag{7}$$

introduced to smooth the transition between the enhanced tropical diffusivity D_t and the weaker extratropical diffusivity D_x. This parametrization of Hadley cell energy transport is easy to implement numerically. We use it here because it allows us to study the effects of Hadley cell expansions on extratropical temperature gradients without complicating the interpretation of the results. See Mbengue (2015) for a discussion of other Hadley cell parameterizations we have explored, including one similar to the parameterization in Lindzen and Farrell (1981).

Our overall results are not sensitive to details of how the Hadley cell energy transport is formulated. However, the transition width of the top-hat function (7) modifies the sensitivity of the storm tracks to Hadley cell expansions. If the transition between extratropics and tropics is unphysically abrupt, the tropics and extratropics decouple and thus, Hadley cell

expansions push storm tracks poleward only when the Hadley cell terminus is closer to the storm tracks.

d. *Tropical–extratropical transition*

It remains to link the Hadley cell terminus ϕ_h to other quantities in the EBM. The latitude at which the eddy momentum flux divergence (meridional wave activity flux) changes sign corresponds to the latitude at which vertical wave activity fluxes become deep enough to reach the upper troposphere (Korty and Schneider 2008; Ait-Chaalal and Schneider 2015). So an approximation of the Hadley cell terminus can be obtained as the latitude at which the meridional energy fluxes (vertical wave activity fluxes) first reach the tropopause. Building on Held (1978), Schneider and Walker (2006) showed that this is the lowest latitude at which the supercriticality

$$S_c(\phi) = -\frac{f}{\beta}\frac{\partial_y \overline{\theta}_s}{\Delta_v} = -\tan(\phi)\frac{\partial_\phi \overline{\theta}_s}{\Delta_v}, \tag{8}$$

a measure of the depth of baroclinic eddy energy fluxes, first reaches an $O(1)$ value. Here, f is the planetary vorticity, β is the planetary vorticity gradient, $y = R\phi$ is the meridional distance coordinate, θ is potential temperature, and $\Delta_v = -2\,\overline{\partial_p \theta_s}\,(\bar{p}_s - \bar{p}_t)$ is a bulk static stability measure (Schneider and Walker 2006). In a wide range of dry and moist idealized GCM simulations, the supercriticality S_c or moist generalizations thereof indeed take an approximately constant $O(1)$ value at the Hadley cell terminus (Korty and Schneider 2008; O'Gorman 2011; Levine and Schneider 2015).

Thus, we take $S_c = S_{c,h}$, where $S_{c,h}$ is an $O(1)$ constant, as the criterion that determines where the Hadley cell terminates in our EBM. Because

$$\phi_h = \tan^{-1}\left(-S_{c,h}\,\frac{\Delta_v}{\partial_\phi \bar{T}}\right), \tag{9}$$

this implies that the Hadley cell widens when the bulk stability Δ_v at the Hadley cell terminus increases, and it narrows when the meridional temperature gradient $\partial_y \bar{T}$ strengthens. Note that we have replaced the mean potential temperature $\bar{\theta}$ by the mean temperature $\bar{T}$ because

the EBM is written in terms of temperature. This simplification neglects variations in pressure and so evaluates the Hadley cell extent on an isobaric surface. Since $\theta = (p_0/p)^\kappa T$, the constant $S_{c,h}$ absorbs a constant $(p_{ns}/p_0)^\kappa$, where κ is the adiabatic exponent, p_0 is a reference pressure and p_{ns} is a representative near-surface pressure. Therefore, $S_{c,h}$ here is smaller than if it is evaluated with potential temperature gradients. This simplification is justified by how well it predicts the changes in the Hadley terminus in the dry GCM (Fig. 6 below).

We now have a closed set of equations to study storm-track shifts. Solutions of the energy balance equation (1) provide the zonal-mean temperature profile and its derivatives, as functions of time and latitude. The bulk stability is taken to be an adjustable parameter, and the supercriticality is taken to be constant at the Hadley cell terminus.

4. EBM Results

Table 1 lists EBM parameters and their reference values used throughout this study. Most parameter values are the same as those used to force the GCM, especially the radiative parameters. Table 2 details how the EBM parameters were varied to explore the model's sensitivity to them.

a. Analytical solution

An approximate analytical solution of the EBM is possible in a reference frame fixed on the Hadley cell terminus ϕ_h if $D_x \cos(\phi)$ (rather than D_x itself) is taken to be constant (see appendix). The Hadley cell terminus ϕ_h enters the solution as a parameter. In this approximate analytical solution, we specify transient eddy energy fluxes F, or the meridional temperature gradient $\partial_y T = -F/D$, at the Hadley cell terminus, which serves as a boundary condition on the extratropical temperature profile. The analytical solution does not contain any Hadley cell parameterization, since iterations would then be necessary to enforce con-

tinuous temperatures and temperature gradients at the Hadley cell terminus. Nonetheless, much insight is possible even without the explicit Hadley circulation parametrization that is contained in the full EBM.

For a two-mode spectral approximation of the analytical solution, Fig. 2a shows the response of zonal-mean temperatures outside the Hadley cell to changes in the subtropical eddy energy fluxes F at the Hadley cell terminus (left) and to changes in the eddy efficiency $\zeta \propto \tau_{\mathrm{rad}} D/R^2$ (right), which measures the eddy mixing efficiency relative to the radiative relaxation (Held 1999). Figure 2b shows the corresponding response of the zonal-mean meridional temperature gradient profile, while Fig. 2c shows the zonal-mean meridional temperature curvature profile. Storm tracks are identified as maxima of the magnitude of the meridional temperature gradient, that is, as extrema of the meridional eddy energy flux weighted by the cosine of latitude (Fig. 2b). That means they coincide with zeros of the meridional energy flux convergence, or zeros of the meridional curvature of the temperature profile (Fig. 2c). As the temperature gradient at and thus the transient eddy energy flux across the boundary of the Hadley cell strengthen, storm tracks (temperature gradient or energy flux extrema) shift equatorward. The equatorward shift occurs because the boundary condition of zero meridional temperature gradients at the pole implies that inflection points of the temperature profile (extrema of the gradient) shift equatorward as eddy energy fluxes across the Hadley cell terminus strengthen.

More precisely, the approximate analytical solution shows that to first order, the difference between the storm track latitude ϕ_s and the Hadley cell terminus ϕ_h is given by

$$\phi_s - \phi_h \approx \frac{8}{R(1+\zeta)} E_x \left(\frac{F}{D}\right)^{-1} - \frac{8}{3\pi^2}\frac{4+\zeta}{1+\zeta}(\pi/2 - \phi_h), \tag{10}$$

where E_x is an average extratropical radiative-equilibrium temperature. The signs were chosen for the northern hemisphere (positive latitudes). This expression shows that storm tracks move closer to the Hadley cell terminus if transient eddy energy fluxes F or temperature gradients $\partial_y T = -F/D$ at the Hadley cell terminus strengthen. Increasing the eddy efficiency ζ also reduces the distance between storm tracks and Hadley cell terminus at fixed

temperature gradients at the Hadley cell terminus (Fig. 2, right), and it makes the distance less sensitive to variations in the temperature gradient at the terminus. The second term on the right-hand side of (10) prevents the distance between Hadley cell terminus and storm track from exceeding the distance between the Hadley cell terminus and the pole; thus, it depends on the Hadley cell terminus ϕ_h, as does the eddy efficiency ζ, where the distance between Hadley cell terminus and pole enters in the non-dimensionalization of the diffusivity (see appendix). Figure 3 illustrates how the distance $\phi_s - \phi_h$ varies with eddy energy flux F at the Hadley cell terminus for different eddy efficiencies ζ, for the complete analytical solution of the EBM (2 spectral modes) with constant $D_x \cos(\phi)$ and for the first-order (10) and a second-order (A16) approximations. The Hadley cell terminus ϕ_h is taken to be constant in the analytical solutions, although in reality, it also depends on the subtropical temperature gradient.

These results demonstrate two distinct modes of storm-track shifts:

i. Storm tracks can shift through changes in the transient eddy energy flux or the temperature gradient at the Hadley cell terminus. A strengthening of the poleward transient eddy energy flux or of the temperature gradient at the Hadley cell terminus generally leads to a shift of storm tracks toward the Hadley cell terminus, and a weakening to a shift away from the terminus—unless compensated, for example, by changes in eddy efficiency or in average extratropical radiative-equilibrium temperature E_x.

ii. Storm tracks can shift with the Hadley cell terminus. If, for example, the static stability in the subtropics changes, the Hadley cell terminus can shift, leading to a concomitant shift of the storm tracks provided changes in the transient eddy energy flux across the Hadley cell terminus or in the eddy efficiency do not modulate the Hadley cell–storm track distance sufficiently to compensate. This is a mechanism through which tropical processes (e.g., changes in tropical convective stability) can influence storm-track position. It is worth noting that the average extratropical radiative-equilibrium temperature E_x depends on the Hadley cell terminus ϕ_h. Thus, poleward storm-track

shifts driven by Hadley cell expansions can be compensated by equatorward shifts due to decreases in E_x.

These two modes of storm track shifts arise out of the EBM dynamics and exist independently of changes, for example, in eddy diffusivities or eddy efficiencies. For example, a change in the eddy length scale, as proposed previously (Kidston et al. 2010), is not necessary; changes in transient eddy energy fluxes across the Hadley cell terminus suffice, however they arise. But our results do not rule out that changes in eddy length scales or other factors may still be important for storm track shifts.

b. Numerical simulations

We solve the complete set of EBM equations numerically with second-order central differences in space, with 1° resolution. The simulations are advanced in time using forward Euler time stepping, until a steady state is reached. The simulations advance as follows: (1) Given a temperature profile as a function of latitude, ϕ_h is calculated as the first latitude where the supercriticality (8) exceeds a critical value; (2) the diffusivity is calculated based on (6); (3) the model is integrated one step forward in time using (1); (4) this sequence is iterated in the next time step.

1) Sensitivity to tropical stability variations

To relate the Hadley cell extent to the convective lapse rate in the tropics, we need to relate Δ_v to the convective rescaling parameter γ. Assuming that hydrostatic equilibrium holds and that the convective lapse rate $\gamma\Gamma_d$ prevails throughout the tropics, we deduce that $\partial_p\theta = -(\theta/T)(\Gamma_d - \gamma\Gamma_d)/(\rho g)$. Hence, the tropical bulk stability is given by

$$\Delta_v = \frac{2(1-\gamma)(p_s - p_t)\theta}{\rho c_p T}, \tag{11}$$

and we assume the subtropical bulk stability at the Hadley cell terminus to scale with the tropical bulk stability. In using (11), we assume that $T \approx \theta$. Thus, we can analytically relate variations in γ to variations in the bulk stability Δ_v at the Hadley cell terminus and, given the temperature gradient at the terminus, to the Hadley cell extent via the supercriticality criterion (9). For fixed meridional temperature gradients and supercriticality at the Hadley cell terminus, increasing the bulk stability leads to a poleward expansion of the Hadley cell.

The response of the Hadley cell terminus and the storm tracks in the EBM to changes in the convective stability are shown in Fig. 4. The EBM's response is qualitatively similar to the response seen in the GCM (Fig. 1b): as the convective stability increases, the midlatitude storm tracks migrate poleward, generally in tandem with the Hadley cell terminus. This suggests that the EBM captures important mechanisms controlling storm-track shifts in response to deep-tropical convective-stability variations. The storm tracks in this case are essentially being forced poleward by an expanding Hadley circulation. As the Hadley cell expands, maximum temperature gradients are expelled further poleward—the second mode of storm track shifts highlighted above.

In low-convective stability climates in the EBM, the distance from the storm tracks to the Hadley cell terminus is too great for the expansion of the Hadley cell to be communicated through midlatitude eddies (Fig. 4, simulations with large γ). The shift of the Hadley cell terminus decouples from the storm track shift. A similar behavior is seen in the GCM at low convective stability (see MS13 or Fig. 1b). In the range $\gamma \leq 0.88$, synoptic eddies begin to feel the influence of the expanding Hadley cell and migrate poleward with it.

Forced on its own, the EBM produces results that are qualitatively similar to the GCM, supporting the hypothesis that shifts in the Hadley cell terminus can push storm tracks poleward.

2) Comparing EBM to GCM

For a more direct comparison of EBM with GCM results, we take the subtropical bulk stability from zonal-mean statistics in the GCM simulations and then solve the EBM numerically with the given bulk stability, specifying the diffusivity as in (6), with the tropical diffusivity D_t taken to be 10^7 m^2 s^{-1} and the extratropical diffusivity D_x is taken to be half of the GCM's extratropical-mean diffusivity, in order for the EBM's and GCM's maximum extratropical temperature gradient to match. The extratropical diffusivity D_x is usually around 2×10^6 m^2 s^{-1}. Additionally, we use the global-mean temperature from the GCM as the EBM's mean radiative-equilibrium temperature $\bar{T}_E$. The EBM and GCM are forced in the same way and occupy different positions in a model hierarchy, with the EBM elucidating causes of the storm track shifts seen in the GCM simulations.

Figure 5 compares a statistically steady state climate from the GCM to the corresponding EBM result. The zonal-mean temperature profiles agree qualitatively (Fig. 5a). The errors in the extratropics are largest near the poles, where variations of the effective diffusivity with latitude play a sizable role. There are also substantial errors in the deep tropics: for example, the EBM's temperatures are biased low relative to the GCM's—although they both have the same global-mean temperature. This is because a near-surface thermally-indirect circulation, not taken into account in the EBM, reverses temperature gradients near the equator in the GCM. In simulations where there is no such near-surface circulation, there is a closer correspondence between the EBM and the GCM in the tropics—but the errors at the pole remain because the constant-diffusivity parameterization is inadequate there.

Although the EBM with its constant diffusivity in the extratropics is too simple to capture the rich structure of the GCM's temperature gradient profile (Fig. 5b), it does capture the position of the storm track, and the Hadley cell parameterization seems to work adequately. The EBM captures the salient features of the GCM's mean-temperature and temperature-gradient profile. The storm track latitudes in the EBM and GCM roughly coincide if the tropical and extratropical diffusivities derived from the GCM are used in the EBM.

Figure 6a compares storm-track and Hadley-terminus responses to variations in tropical convective stability. Here, the EBM is forced with variables computed from the GCM: the mean temperature, average extratropical diffusivity (averaged between the Hadley terminus and 60N), and bulk stability are all taken from GCM simulations in which the deep-tropical convective stability is varied. The diffusivity within the Hadley cell is set to a constant $D_t = 10^7$ m^2 s^{-1}. The analytical solution for the storm track latitude given the Hadley cell terminus latitude, with parameters as in the full EBM, is also shown in the figure. As the tropical convective stability increases, the Hadley cell expands and the storm tracks shift poleward, in tandem with the Hadley cell terminus. With a constant tropical diffusivity D_t, storm tracks in the EBM sit $5.5° \pm 0.9°$ poleward of the storm tracks in the GCM. This is because, as explained earlier, thermally indirect circulations in the deep tropics in the GCM lead to steeper subtropical temperature gradients in the GCM, which are not captured in the EBM. Figure 6 also reveals that the supercriticality criterion (9) in the EBM captures changes in the Hadley cell extent in the GCM very well. Figure 6b is the same as in Fig. 6a but instead uses an average tropical diffusivity D_t computed for each GCM simulation individually (by averaging fluxes and gradients between 10°N and the Hadley cell terminus). The fit between the storm tracks in the EBM and GCM is improved, albeit with a slight degradation in the Hadley terminus fit.

Figure 7 compares the relationship between the subtropical temperature gradients and the differences between storm-track latitude and the Hadley cell terminus, in the EBM, GCM, and analytical solution of the EBM. What are plotted are the anomalies around the arithmetic mean for each dataset. There is a clear monotonic relationship between subtropical temperature gradients and the distance between the storm tracks and the Hadley cell terminus. In the EBM using the GCM's tropical diffusivity, storm tracks move away from the Hadley cell terminus at 0.27°–0.31° per Kelvin strengthening of subtropical temperature gradients (where temperature gradients are multiplied by Earth's radius R to express them as temperature differences). In the GCM, the dependence of storm track distance to Hadley cell

terminus on subtropical temperature gradients is, within the statistical uncertainty, similar (0.19°–0.71° per K), and it is also similar for the analytical solution to the EBM (0.23°–0.85° per K). Much of the spread in the GCM results around the regression line comes from noise in estimating subtropical temperature gradients from the GCM. Overall, however, changes in the subtropical temperature gradient and in the flux across the Hadley cell terminus account for only a small fraction of the variance in the storm-track latitude. The shifts in the storm-track latitude in these simulations are dominated by shifts in the Hadley terminus.

5. Discussion and conclusions

We have developed an EBM with an explicit representation of Hadley cell energy transport to illustrate how the storm track position can be dynamically coupled to Hadley cell dynamics. A key ingredient of this coupling is that the Hadley cell terminates where a baroclinicity measure, which depends on the meridional temperature gradient and a bulk static stability, first exceeds a critical value. The meridional temperature gradient at the Hadley cell terminus, in turn, determines the eddy energy export out of the Hadley cell into the extratropics, and its strength controls the distance between the Hadley cell terminus and the storm tracks, identified as extrema in the meridional temperature gradient or zeros of the meridional eddy energy flux divergence.

While this EBM is simple conceptually, it exhibits rich behavior, which can help explain how the storm track position varies as various climatic factors are varied. Two distinct modes of storm track shifts emerge: (1) Storm tracks move closer to the Hadley cell as the meridional temperature gradient, or transient eddy energy flux, at the Hadley cell terminus strengthen. This is a result of the diffusive nature of the EBM, which leads to an inflection point in the meridional temperature profile closer to the Hadley cell terminus when subtropical temperature gradients strengthen. (2) Storm tracks shift in tandem with the Hadley cell terminus, as long as changes in the transient eddy energy export out of the Hadley cell (and

parameters such as the diffusivity) stay fixed. This is a result of the dynamical coupling between the latitude of the Hadley cell terminus and meridional temperature gradients in the extratropics, whose extrema coincide with the storm tracks.

Both modes of storm track shifts can be demonstrated in the EBM, both in analytical and numerical solutions, and they are also seen in the simulations with an idealized GCM we published earlier (MS13 and MS17). In particular, most variations in storm track latitude in the GCM are accounted for by variations in the Hadley cell terminus. These can arise entirely by tropical processes. For example, an increase in the convective stability only in the deep tropics leads to a widening of the Hadley cell by increasing the bulk stability throughout the tropics (MS13), thus leading to a poleward shift of the latitude where the baroclinicity measure first exceeds its critical value. This poleward expansion of the Hadley cell pushes extratropical temperature gradients and thus storm tracks poleward, because the distance of storm tracks to the Hadley cell terminus, for a given diffusivity, depends on the meridional temperature gradient at the Hadley cell terminus as a boundary condition. Such changes in the Hadley cell terminus can arise through a variety of processes and account for most of the shifts in storm track latitude seen in the GCM simulations (mode 2 above). Additionally, changes in the meridional temperature gradient at the Hadley cell terminus lead to changes in the distance between storm tracks and the Hadley cell terminus, which account for a smaller portion of the shifts in storm track latitude seen in the GCM simulations (mode 1 above).

Our results at least qualitatively provide a unifying conceptual model for various ways in which storm tracks can shift that have been described in the literature:

- Idealized and comprehensive climate models show a robust poleward shift of storm tracks as the climate warms globally (Yin 2005; Bengtsson et al. 2006; Hu and Fu 2007; Lu et al. 2007; Seidel et al. 2008; Barnes and Polvani 2013; Mbengue and Schneider 2013; Adam et al. 2014; Levine and Schneider 2015). Generally, the storm tracks shift in tandem with the Hadley cell terminus (Kang and Polvani 2011; Ceppi and Hartmann

2013; Mbengue and Schneider 2013). Our EBM likewise predicts a poleward shift of storm tracks under global warming through expansions of the Hadley cell primarily driven by increased tropical static stability (mode 2).

- In contrast to the global-warming response, storm tracks migrate equatorward during the El Niño phase of the Southern Oscillation (Chang et al. 2002; Seager et al. 2003; Lu et al. 2008; Tandon et al. 2013; Adam et al. 2014). During El Niño, subtropical meridional temperature gradients strengthen, which can lead to the contraction of the Hadley cell because the subtropical baroclinicity (supercriticality) increases. Consistent with our EBM, storm tracks shift equatorward, most likely primarily with the Hadley cell terminus (mode 2). It is an open and interesting question whether an additional storm track shift toward the Hadley cell (mode 1) can also be extracted from observations.

- Idealized GCM simulations aimed at elucidating the differences between the global-warming and El Niño responses of the atmospheric circulation have shown equatorward storm-track shifts for narrow tropical heating or strengthened subtropical temperature gradients, and poleward storm-track shifts for broad tropical or midlatitude heating (Chang 1995; Butler et al. 2010; Tandon et al. 2013; Sun et al. 2013). Such storm-track shifts are consistent with the modes 1 and 2 mechanisms discussed here. For example, narrow tropical heating strengthens subtropical temperature gradients and leads to a contraction of the Hadley cell, implying an equatorward storm-track shift both because the Hadley cell contracts and possibly also because temperature gradients at the Hadley cell terminus strengthen. On the other hand, broad tropical heating increases the subtropical bulk stability, leading to an expansion of the Hadley circulation and a concomitant poleward storm track shift.

- In idealized GCM simulations, storm tracks have been seen to move closer to the Hadley cell as subtropical temperature gradients strengthen and away from it as subtropical

temperature gradients weaken (Brayshaw et al. 2008; Tandon et al. 2013)—like in our EBM and dry GCM simulations.

- Idealized and comprehensive GCM simulations have shown that storm tracks shift poleward as the tropopause height increases (Schneider 2004; Williams 2006; Lorenz and DeWeaver 2007). The same occurs in our EBM and dry GCM because an increased tropopause height implies an increased bulk stability in the subtropics and thus an expansion of the Hadley cell, which pushes storm tracks poleward.

- The EBM, in concert with our previous GCM studies, is consistent with the finding that variations in lower-tropospheric meridional temperature gradients account for much of the spread in storm track positions seen in comprehensive GCM simulations (Harvey et al. 2015).

Our EBM notably does not represent upper-tropospheric eddy momentum fluxes explicitly, except insofar as that the eddy momentum fluxes are viewed as essential for terminating the Hadley cell where their divergence changes sign, which occurs where the vertical wave activity fluxes become deep enough to reach the upper troposphere (Korty and Schneider 2008). It has been postulated that changes in eddy phase speeds that modulate where eddies break and eddy momentum fluxes change sign can drive changes in the Hadley cell terminus and in storm track latitude (Chen and Held 2007). While that remains a possibility, from the perspective of the EBM, the upper-tropospheric eddy momentum fluxes adjust to, rather than drive, changes in the lower-tropospheric eddy energy fluxes (vertical wave activity fluxes) and temperature gradients that ultimately determine the storm track position.

To what extent the EBM can quantitatively account for storm track shifts by a variety of disparate mechanisms remains to be investigated. It is possible that variations of the diffusivity/eddy efficiency with latitude and climate may need to be taken into account to quantitatively account for some of the shifts seen in observations and simulations. It is also to be kept in mind that storm tracks are strongly influenced by stationary eddy

546 activity (Kaspi and Schneider 2011, 2013; Simpson et al. 2014; Shaw and Voigt 2015), which
547 are not explicitly taken into account in our EBM. Additionally, moisture and latent heat
548 release affect the eddy efficiency and static stability (Flannery 1984; Held 1993; Caballero
549 and Langen 2005; O'Gorman and Schneider 2008; Schneider and Bordoni 2008; O'Gorman
550 2011; Cabellero and Hanley 2012)—effects that currently are not considered in our EBM but
551 may be captured with suitable generalizations of the bulk stability or the energy flux that is
552 represented by the EBM. The EBM and the two modes of storm-track shifts it exhibits are
553 a useful starting point to anchor such further investigations.

Acknowledgments.

We are grateful for the financial support of the National Science Foundation (grant AGS-1019211). We also thank Xavier Levine for several helpful discussions and for his comments on an early draft of this work.

APPENDIX

Analytical EBM Solution

Starting with the steady-state version of the EBM equation and assuming $D\cos\phi$ to be constant, we obtain a Cartesian ODE,

$$D\partial_{yy}T - A\big[T - E(y)\big] = 0, \tag{A1}$$

where $y = R\phi$ and $A = 1/\tau_{\rm rad}$. The boundary conditions are a specified energy flux F across the Hadley terminus at distance $y_h = R\phi_h$ from the equator, and zero flux at the pole:

$$\begin{aligned} \partial_y T(y_h) &= -F/D \\ \partial_y T(R\pi/2) &= 0. \end{aligned} \tag{A2}$$

Focusing on the northern hemisphere for notational simplicity, we nondimensionalize the domain using $y' = \alpha(y - y_h)$, where $\alpha = (y_p - y_h)^{-1}$ with distance to pole $y_p = R\pi/2$, so that the Hadley cell terminus is at $y' = 0$ and the north pole at $y' = 1$. The radiative-equilibrium temperature profile is transformed accordingly to

$$E(y') = \bar{T}_E + \Delta_H \left\{1/3 - \sin^2\left([\alpha^{-1}y' + y_h]/R\right)\right\}. \tag{A3}$$

The ODE becomes

$$D'\partial_{y'y'}T - A\big[T - E(y')\big] = 0, \tag{A4}$$

where $D' = \alpha^2 D$, with boundary conditions,

$$\partial_{y'} T(0) = -\alpha F / D'$$
$$\partial_{y'} T(1) = 0. \tag{A5}$$

The EBM equation subject to the boundary conditions and the assumptions above can be solved analytically. First, we homogenize boundary conditions by defining a new temperature, $T = T' + w$, where $w = -2\alpha F/(\pi D') \sin(\pi y'/2)$. This yields the transformed equation

$$\left[D' \partial_{y'y'} - A\right] T' + S' = 0, \tag{A6}$$

with homogeneous boundary conditions

$$\partial_{y'} T'(0) = 0,$$
$$\partial_{y'} T'(1) = 0, \tag{A7}$$

where $S' = AE - (A + \pi^2 D'/4)\, w$, or

$$S' = AE + \frac{\pi \alpha B F}{2} \sin\left(\frac{\pi y'}{2}\right), \tag{A8}$$

with

$$B = \left(\frac{4A}{\pi^2 D'} + 1\right) \tag{A9}$$

as a measure of radiative forcing strength relative to eddy diffusion. This boundary value problem has cosines as eigenfunctions, so we express the solution as a cosine series, $T' = \sum_{n\geq 0} \tau_n \cos(n\pi y')$, and expand the forcing analogously: $S' = \sum_{n\geq 0} s_n \cos(n\pi y')$. The solution for temperature follows immediately by substitution, if we assume a small angle approximation for the implicit secant variations of D,

$$T(y') = w + \sum_{n\geq 0} \frac{s_n \cos(n\pi y')}{n^2 \pi^2 D' + A}, \tag{A10}$$

where $s_0 = \int_0^1 S'\, dy'$ and $s_n = 2\int_0^1 S' \cos(n\pi y')\, dy'$ for $n > 0$.

A two-mode approximation suffices to illustrate key properties of the solution,

$$T(y') \approx \langle E \rangle + \frac{\alpha B F}{A} + G \cos \pi y' - \frac{2\alpha F}{\pi D'} \sin \frac{\pi y'}{2}, \tag{A11}$$

where

$$G = \frac{2A\langle E \cos(\pi y') \rangle - 2\alpha B F/3}{\pi^2 D' + A} \tag{A12}$$

and the angle brackets denote an integral over y': $\langle \cdot \rangle = \int_0^1 (\cdot)\, dy'$.

The storm-track latitude is obtained by taking the second derivative of this solution with respect to y' and solving for its zeros. Using a first-order Taylor expansion in y', the result is

$$y'_s \approx \frac{4GD'}{\alpha F}, \tag{A13}$$

or, substituting for G and B from their definitions and restoring the original meridional coordinate,

$$y_s - y_h \approx \frac{8}{1+\zeta} \langle E \cos(\pi y') \rangle \left(\frac{F}{D} \right)^{-1} - \frac{8}{3\pi^2} \frac{4+\zeta}{1+\zeta} (y_p - y_h), \tag{A14}$$

where the eddy efficiency $\zeta = \pi^2 \alpha^2 D/A$ measures the relative importance of eddy diffusion to radiative driving. For a fixed Hadley cell terminus latitude ϕ_h (i.e., fixed y_h and α), it is clear from this solution that the storm tracks move closer to the Hadley cell terminus as the energy flux F across the terminus strengthens, or, more precisely, as the temperature gradient ($\propto -F/D$) at the terminus strengthens at fixed ζ. A second-order approximation,

$$y_s - y_h \approx \frac{1}{2} \left(\sqrt{\psi^2 + \frac{8}{\pi^2}} - \psi \right) (y_p - y_h), \tag{A15}$$

where

$$\psi = \frac{3(1+\zeta)}{4(4+\zeta)} \left[\frac{3\pi^2 \alpha \, \langle E \cos(\pi y') \rangle}{4+\zeta} \left(\frac{F}{D} \right)^{-1} - 1 \right]^{-1}, \tag{A16}$$

provides an improved fit (Fig. 3). Equation (A16) shows that ψ increases as the energy flux across the terminus strengthens. The first derivative of (A15) with respect to ψ is negative everywhere except in the limit as ψ goes to infinity, where the derivative goes to zero. Therefore, it is again clear that, for fixed y_h and α, storm tracks move closer to the Hadley cell terminus when the strength of the energy flux across the terminus increases.

REFERENCES

Adam, O., T. Schneider, and N. Harnik, 2014: Role of changes in mean temperatures versus temperature gradients in the recent widening of the Hadley circulation. *Journal of Climate*, **27**, 7450–7461.

Ait-Chaalal, F., and T. Schneider, 2015: Why eddy momentum fluxes are concentrated in the upper troposphere. *Journal of the Atmospheric Sciences*, **72**, 1585–1604.

Barnes, E. A., and L. Polvani, 2013: Response of the midlatitude jets, and of their variability, to increased greenhouse gases in the cmip5 models. *Journal of Climate*, **26 (18)**, 7117–7135.

Bengtsson, L., K. Hodges, and E. Roeckner, 2006: Storm tracks and climate change. *Journal of Climate*, **19**, 3518–3543.

Blackmon, M., 1976: A climatological spectral study of the 500mb geopotential height of the Northern Hemisphere. *Journal of the Atmospheric Sciences*, **33**, 1607–1623.

Blackmon, M., J. Wallace, N. Lau, and S. Mullen, 1977: An observational study of the Northern Hemisphere wintertime circulation. *Journal of the Atmospheric Sciences*, **34**, 1040–1053.

Brayshaw, D., B. Hoskins, and M. Blackburn, 2008: The storm-track response to idealized SST perturbations in an aqua-planet GCM. *Journal of the Atmospheric Sciences*, **65**, 2842–2860.

Budyko, M. I., 1969: The effect of solar radiation variations on the climate of the Earth. *Tellus*, **XXI**, 611–619.

Butler, A., D. Thompson, and T. Birner, 2011: Isentropic slopes, downgradient eddy fluxes, and the extratropical atmospheric circulation response to tropical tropospheric heating. *Journal of the Atmospheric Sciences*, **68**, 2292–2305.

Butler, A. H., W. J. Thompson, and R. Heikes, 2010: The steady-state atmospheric circulation response to climate change-like thermal forcings in a simple general circulation model. *Journal of Climate*, **23**, 3474–3496.

Caballero, R., and P. Langen, 2005: The dynamic range of poleward energy transport in an atmospheric general circulation model. *Geophysical Research Letters*, **32**, L02 705, doi:10.1029/2004GL021 581.

Cabellero, R., and J. Hanley, 2012: Midlatitude eddies, storm-track diffusivity, and poleward moisture transport in warm climates. *Journal of the Atmospheric Sciences*, **69**, 3237–3250.

Ceppi, P., and D. L. Hartmann, 2013: On the speed of the eddy-driven jet and the width of the Hadley cell in the Southern Hemisphere. *Journal of Climate*, **26**, 3450–3465.

Chang, E., S. Lee, and K. Swanson, 2002: Storm track dynamics. *Journal of Climate*, **15**, 2163–2183.

Chang, E. K. M., 1995: The influence of Hadley circulation intensity changes on extratropical climate in an idealized model. *Journal of the Atmospheric Sciences*, **55**, 2006–2024.

Chang, E. K. M., 2013: CMIP5 projection of significant reduction in extratropical cyclone activity over North America. *Journal of Climate*, **26**, 9903–9922.

Charney, J. G., 1963: A note on large-scale motions in the tropics. *Journal of the Atmospheric Sciences*, **20 (6)**, 607–609.

Chen, G., and I. Held, 2007: Phase speed spectra and the recent poleward shift of Southern Hemisphere surface westerlies. *Geophysical Research Letters*, **34**, L21 805, doi:10.1029/2007GL031 200.

Chen, G., J. Lu, and D. Frierson, 2008: Phase speed spectra and the latitude of surface westerlies: interannual variability and global-warming trend. *Journal of Climate*, **21**, 5942–5959.

Corrsin, S., 1974: Limitations of gradient transport models in random walks and in turbulence. *Advances in Geophysics*, **18A**, 25–60, academic Press.

Flannery, B. P., 1984: Energy balance models incorporating transport of thermal and latent energy. *Journal of the Atmospheric Sciences*, **41 (3)**, 414–421.

Frierson, D. M. W., I. M. Held, and P. Zurita-Gotor, 2007a: A gray-radiation aquaplanet moist GCM. Part II: energy transports in altered climates. *Journal of the Atmospheric Sciences*, **64**, 1680–1693.

Frierson, D. M. W., J. Lu, and G. Chen, 2007b: Width of the hadley cell in simple and comprehensive general circulation models. *Geophys. Res. Lett.*, **34**.

Geng, Q., and M. Sugi, 2003: Possible change of extratropical cyclone activity due to enhanced greenhouse gases and sulfate aerosols—study with a high resolution AGCM. *Journal of Climate*, **16**, 2262–2274.

Harvey, B. J., L. C. Shaffrey, and T. J. Woollings, 2015: Deconstructing the climate change response of the northern hemisphere wintertime storm tracks. *Climate Dyn.*, doi:10.1007/s00382-015-2510-8.

Held, I. M., 1978: The vertical scale of an unstable baroclinic wave and its importance for eddy heat flux parameterizations. *J. Atmos. Sci.*, **35**, 572–576.

Held, I. M., 1993: Large-scale dynamics and global warming. *BAMS*, **74 (2)**, 228–241.

Held, I. M., 1999: The macroturbulence of the troposphere. *Tellus*, **51A**, 59–70, doi:10.1175/1520-0469(1996)053⟨0946:ASTFHH⟩2.0.CO;2.

Held, I. M., and A. Y. Hou, 1980: Nonlinear axially symmetric circulations in a nearly inviscid atmosphere. *Journal of the Atmospheric Sciences*, **37**, 515–533.

Held, I. M., and M. J. Suarez, 1974: Simple albedo feedback models of the icecaps. *Tellus*, **26 (6)**, 613–629.

Hoskins, B., and K. Hodges, 2002: New perspectives on the Northern Hemisphere winter storm tracks. *Journal of the Atmospheric Sciences*, **59**, 1041–1061.

Hoskins, B. J., and P. J. Valdes, 1990: On the existence of storm-tracks. *Journal of the Atmospheric Sciences*, **47**, 1854–1864.

Hu, Y., and Q. Fu, 2007: Observed poleward expansion of the Hadley circulation since 1979. *Atmos. Chem. Phys.*, **7**, 5229–5236.

Kang, S., and L. M. Polvani, 2011: The interannual relationship between the latitude of the eddy-driven jet and the edge of the Hadley cell. *Journal of Climate*, **24**, 563–568.

Kaspi, Y., and T. Schneider, 2011: Downstream self-destruction of storm tracks. *Journal of the Atmospheric Sciences*, **68**, 2459–2464.

Kaspi, Y., and T. Schneider, 2013: The role of stationary eddies in shaping midlatitude storm tracks. *Journal of the Atmospheric Sciences*, **70**, 2596–2613.

Kidston, J., S. M. Dean, J. A. Renwick, and G. K. Vallis, 2010: A robust increase in the eddy length scale in the simulation of future climates. *Geophysical Research Letters*, **37**, L03 806, doi:10.1029/2009GL041 615.

Korty, R. L., and T. Schneider, 2008: Extent of Hadley circulations in dry atmospheres. *Geophysical Research Letters*, **35, L23803, doi:10.1029/2008GL035847**.

Kushner, P. J., and I. M. Held, 1998: A test, using atmospheric data, of a method for estimating oceanic eddy diffusivity. *Geophysical Research Letters*, **25 (22)**, 4213–4216.

693 Kushner, P. J., and L. M. Polvani, 2004: Stratosphere-troposphere coupling in a relatively
694 simple AGCM: the role of eddies. *Journal of Climate*, **17**, 629–639.

695 Levine, X., and T. Schneider, 2015: Baroclinic eddies and the extent of the Hadley circu-
696 lation: an idealized GCM study. *Journal of the Atmospheric Sciences*, **72**, 2744–2761,
697 doi:https://doi.org/10.1175/JAS-D-14-0152.1.

698 Lindzen, R. S., and B. Farrell, 1977: Some realistic modifications of simple climate models.
699 *Journal of the Atmospheric Sciences*, **34**, 1487–1501.

700 Lindzen, R. S., and B. Farrell, 1981: The role of polar regions in global climate, and a new
701 parameterization of global heat transport. *Monthly Weather Review*, **108**, 2064–2079.

702 Lorenz, D., 2014: Understanding midlatitude jet variability and change using Rossby wave
703 chromatography: poleward-shifted jets in response to external forcing. *Journal of the*
704 *Atmospheric Sciences*, **71**, 2370–2389.

705 Lorenz, D. J., and E. T. DeWeaver, 2007: Tropopause height and zonal wind response to
706 global warming in the IPCC scenario integrations. *Journal of Geophysical Research*, **112**,
707 D10 119, doi:10.1029/2006JD008 087.

708 Lorenz, E. N., 1979: Forced and free variations of weather and climate. *Journal of the*
709 *Atmospheric Sciences*, **36**, 1367–1376.

710 Lu, J., G. Chen, and D. Frierson, 2010: The position of the midlatitude storm track and
711 eddy-driven westerlies in aquaplanet AGCM. *Journal of the Atmospheric Sciences*, **67**,
712 3984–4000.

713 Lu, J., G. Chen, and D. M. W. Frierson, 2008: Response of the zonal mean atmospheric
714 circulation to el niño versus global warming. *J. Climate*, **21**, 5835–5851.

715 Lu, J., A. G. Vecchi, and T. Reichler, 2007: Expansion of the Hadley cell under global
716 warming. *Geophysical Research Letters*, **34**, doi: 10.1029/2006GL028 443.

Mbengue, C., and T. Schneider, 2013: Storm track shifts under climate change: what can be learned from large-scale dry dynamics. *Journal of Climate*, **26**, 9923–9930.

Mbengue, C., and T. Schneider, 2017: Storm-track shifts under climate change: toward a mechanistic understanding using baroclinic mean available potential energy. *Journal of the Atmospheric Sciences*, 93–110, doi:10.1175/JAS-D-15-0267.1, URL http://dx.doi.org/10.1175/JAS-D-15-0267.1.

Mbengue, C. O., 2015: Storm track response to perturbations in climate. Ph.D. thesis, California Institute of Technology, available from http://resolver.caltech.edu/CaltechTHESIS:05112015-075223217.

Murray, R. J., and I. Simmonds, 1991: A numerical scheme for tracking cyclone centers from digital data. Part I: development and operation of the scheme. *Aust Met. Mag.*, **39**, 155–166.

North, G. R., 1975a: Analytical solution to a simple climate model with diffusive heat transport. *Journal of the Atmospheric Sciences*, **32**, 1301–1307.

North, G. R., 1975b: Theory of energy-balance climate models. *Journal of the Atmospheric Sciences*, **32**, 2033–2043.

North, G. R., R. F. Cahalan, and J. A. Coakley, 1981: Energy balance climate models. *Reviews of Geophysics and Space Physics*, **19 (1)**, 91–121.

O'Gorman, P., 2010: Understanding the varied response of the extratropical storm tracks to climate change. *PNAS*, **107 (45)**, 19 176–19 180.

O'Gorman, P., 2011: The effective static stability experienced by eddies in a moist atmosphere. *Journal of the Atmospheric Sciences*, **68**, 75–90.

O'Gorman, P., and T. Schneider, 2008: The hydrological cycle over a wide range of climates simulated with an idealized GCM. *Journal of Climate*, **21**, 3815–3832.

O'Gorman, P. A., and T. Schneider, 2006: Stochastic models for the kinematics of moisture transport and condensation in homogeneous turbulent flows. *J. Atmos. Sci.*, **63**, 2992–3005.

Peixoto, J. P., and A. H. Oort, 1992: *Physics of Climate*. Springer-Verlag, NY, USA.

Pierrehumbert, R. T., 2002: The hydrologic cycle in deep-time climate problems. *Nature*, **419**, 191–198.

Pierrehumbert, R. T., H. Brogniez, and R. Roca, 2007: On the relative humidity of the atmosphere. *The Global Circulation of the Atmosphere*, T. Schneider, and A. H. Sobel, Eds., Princeton University Press, Princeton, NJ, 143–185.

Riviere, G., 2011: A dynamical interpretation of the poleward shift of the jet streams in global-warming scenarios. *Journal of the Atmospheric Sciences*, **68**, 1253–1272.

Roe, G. H., N. Feldl, K. C. Armour, Y. Hwang, and D. M. W. Frierson, 2015: The remote impacts of climate feedbacks on regional climate predictability. *Nature Geosci.*, **8**, 135–139.

Roe, G. H., and R. S. Lindzen, 2001: A one-dimensional model for the interaction between continental-scale ice sheets and atmospheric stationary waves. *Climate Dynamics*, **17**, 479–487.

Schneider, E. K., 1977: Axially symmetric steady-state models of the basic state for instability and climate studies. part ii: Nonlinear calculations. *Journal of the Atmospheric Sciences*, **34**, 280–296.

Schneider, E. K., and R. S. Lindzen, 1977: Axially symmetric steady-state models of the basic state for instability and climate studies. part i: Linear calculations. *Journal of the Atmospheric Sciences*, **34**, 263–279.

Schneider, T., 2004: The tropopause and the thermal stratification in the extratropics of a dry atmosphere. *Journal of the Atmospheric Sciences*, **61**, 1317–1340.

765 Schneider, T., T. Bischoff, and H. Potka, 2015: Physics of changes in synoptic midlatitude
766 temperature variability. *Journal of Climate*, **28 (6)**, 2312–2331.

767 Schneider, T., and S. Bordoni, 2008: Eddy-mediated regime transitions in the seasonal cycle
768 of a Hadley circulation and implications for monsoon dynamics. *Journal of the Atmospheric*
769 *Sciences*, **65**, 915–934.

770 Schneider, T., P. O'Gorman, and X. Levine, 2010: Water vapor and the dynamics of climate
771 changes. *Reviews of Geophysics*, **48**, RG3001, doi:10.1029/2009RG000 302.

772 Schneider, T., and C. Walker, 2006: Self-organization of atmospheric macroturbulence into
773 critical states of weak nonlinear eddy-eddy interactions. *Journal of the Atmospheric Sci-*
774 *ences*, **63**, 1569–1586.

775 Schneider, T., and C. Walker, 2008: Scaling laws and regime transitions of macroturbulence
776 in dry atmospheres. *Journal of the Atmospheric Sciences*, **65**, 2153–2173.

777 Seager, R., N. Harnik, Y. Kushnir, W. Robinson, and J. Miller, 2003: Mechanisms of hemi-
778 spherically symmetric climate variability. *J. Climate*, **16**, 2960–2978.

779 Seidel, D. J., Q. Fu, W. J. Randel, and T. J. Reichler, 2008: Widening of the tropical belt
780 in a changing climate. *Nature Geosci.*, **1**, 21–24.

781 Sellers, W. D., 1969: A global climatic model based on the energy balance of the Earth-
782 atmosphere system. *Journal of Applied Meteorology*, **8**, 392–400.

783 Shaw, T., and A. Voigt, 2015: Tug of war on summertime circulation between radiative
784 forcing and sea surface warming. *Nature Geoscience*, **8**, 560–566.

785 Simpson, I. R., T. A. Shaw, and R. Seager, 2014: A diagnosis of the seasonally and lon-
786 gitudinally varying midlatitude circulation response to global warming. *Journal of the*
787 *Atmospheric Sciences*, **71 (7)**, 2489–2515.

Sobel, A. H., J. Nilsson, and L. M. Polvani, 2001: The weak temperature gradient approximation and balanced tropical moisture waves. *J. Atmos. Sci.*, **58**, 3650–3665.

Sun, L., G. Chen, and J. Lu, 2013: Sensitivities and mechanisms of the zonal mean atmospheric circulation response to tropical warming. *Journal of the Atmospheric Sciences*, **70**, 2487–2504.

Swanson, K. L., and R. T. Pierrehumbert, 1997: Lower-tropospheric heat transport in the Pacific storm track. *J. Atmos. Sci.*, **54**, 1533–1543.

Tandon, N. F., E. P. Gerber, A. H. Sobel, and L. M. Polvani, 2013: Understanding Hadley cell expansion versus contraction: Insights from simplified models and implications for recent observations. *Journal of Climate*, **26**, 4304–4321.

Ulbrich, U., J. G. Pinto, H. Kupfer, G. C. Leckebusch, T. Spangehl, and M. Reyers, 2008: Changing northern hemisphere storm tracks in an ensemble of ipcc climate change simulations. *Journal of Climate*, **21 (8)**, 1669–1679.

Walker, C. C., and T. Schneider, 2006: Eddy influences on hadley circulations: Simulations with an idealized gcm. *Journal of the Atmospheric Sciences*, **63 (12)**, 3333–3350.

Williams, G. P., 2006: Circulation sensitivity to tropopause height. *Journal of the Atmospheric Sciences*, **63**, 1954–1961.

Yin, J., 2005: A consistent poleward shift of the storm track in simulations of 21st-century climate. *Geophysical Research Letters*, **32**, L18 701, doi:10.1029/2005GL023 684.

List of Tables

TABLE 1. Simulation and reference parameters

Parameter	Symbol	Value
	Planet and fluid	
Specific Heat	c_p	1004 J kg^{-1} K^{-1}
Diffusivity	D	2.1×10^6 m^2 s^{-1}
Hadley cell extent	$\phi_{\rm h}$	25°N
Planetary radius	R	6.365×10^6 m
Supercriticality	$S_{c,h}$	0.28
Pressure depth	$p_s - p_t$	700 hPa
Density	ρ	1.0 kg m^{-3}
Convective lapse rate	$\gamma\Gamma_d$	6.9 K km^{-1}
	Diabatic processes	
Radiative-equilibrium mean temperature	$\bar{T}_{eq}$	288 K
Pole-equator temp. contrast	Δ_H	120 K
	Relaxation timescales	
Atmosphere	$\tau_{\rm rad}$	50 days

TABLE 2. Simulation parameters for sensitivity tests using the analytical solution and for the numerical simulations [min : (step) : max]

Experimental Parameter	Symbol	Value
	Sensitivity study with analytical model	
Eddy efficiency	$\zeta' = D'/A = D\tau_{\mathrm{rad}}(R[\pi/2 - \phi_h])^{-2}$	$0.1 : 0.05 : 0.3$
Subtropical northward eddy energy flux	F	$0 : 30$ K m/s
	Numerical simulations	
Convective parameter	γ	$0.6 : 0.02 : 0.98$

List of Figures

857 7 Difference between the latitudes of the storm track ϕ_s and the Hadley terminus
858 ϕ_h versus subtropical temperature gradient, for the EBM (red), the GCM
859 (black), and the analytical EBM solution forced with parameters from the
860 GCM but with the Hadley cell terminus assumed constant at 25°N (blue). The
861 least-squares linear-regression lines are plotted in their respective colors. The
862 temperature gradient has been multiplied by the Earth radius R to express
863 it as a temperature difference in units of Kelvin. What are plotted are the
864 anomalies relative to the arithmetic mean for each dataset. 48

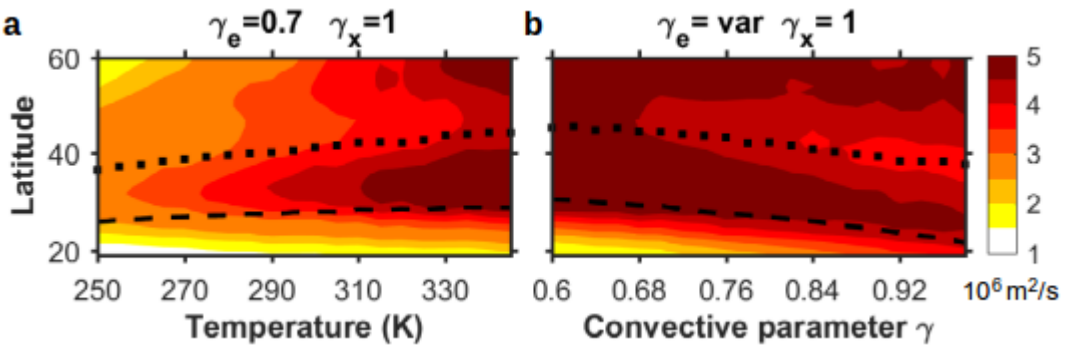

FIG. 1. Near-surface eddy diffusivity $D = -\{\overline{v'\theta'}\}/\{\partial_y\theta\}$ for GCM simulations in which the mean radiative-equilibrium temperature and the tropical convective static stability are varied. (a) Variation of global-mean radiative-equilibrium temperature. Deep-tropical temperatures are relaxed toward a moist adiabatic profile ($\gamma_e = 0.7$), while temperatures outside of this region are relaxed toward a dry adiabat ($\gamma_x = 1$). (b) Variations of deep-tropical static stability (γ_e), while the convective static stability in the extratropics remains dry adiabatic ($\gamma_x = 1$). The dashed line marks the Hadley cell terminus, and the dotted line the storm track.

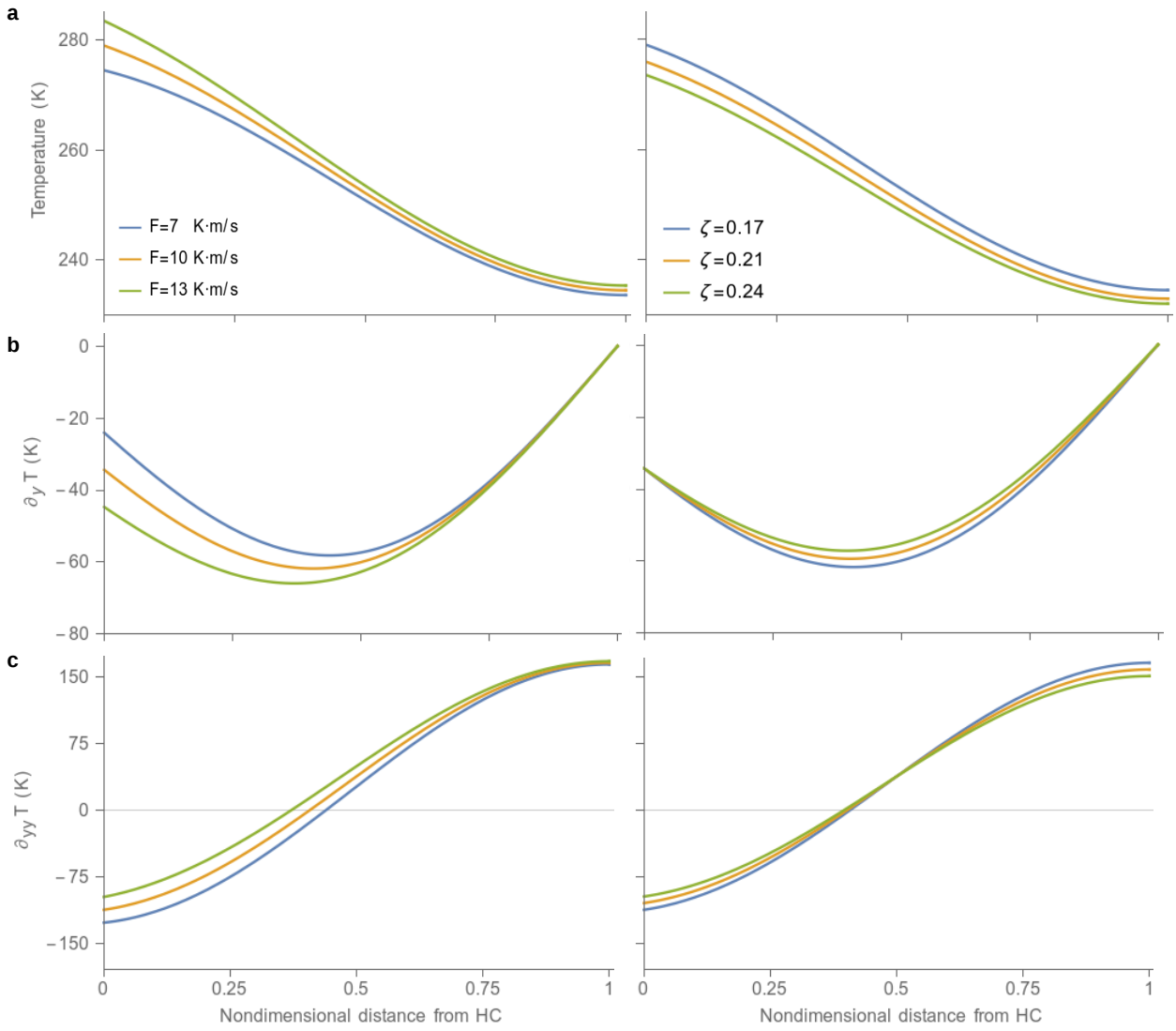

FIG. 2. Two-mode analytical approximations. Left: variations in subtropical energy fluxes for fixed eddy efficiency. Right: variations in eddy efficiency for fixed subtropical energy flux. (a) Zonal-mean temperature profile for a two-mode analytical approximation. (b) Zonal-mean meridional temperature-gradient profile. (c) Zonal-mean meridional temperature-curvature profile. Temperature gradients are multiplied by the Earth radius R and curvatures by R^2 to express them in units of Kelvin. The Hadley cell terminus is at 0 and the pole at 1. Storm tracks are identified as global maxima of the absolute value of near-surface meridional temperature gradients, or as zeros of the temperature curvature. Strengthening the meridional temperature gradient at and thus the energy flux across the Hadley cell terminus shifts the storm tracks toward the Hadley cell terminus. For fixed energy flux across the Hadley cell, increasing the eddy efficiency shifts storm tracks toward the Hadley cell.

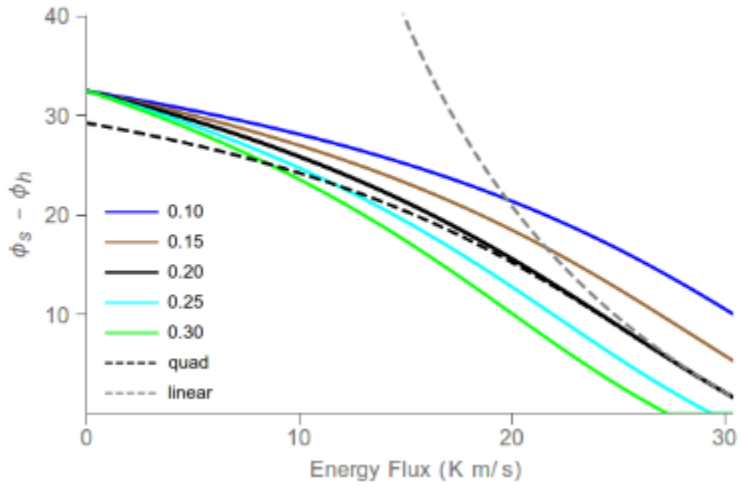

FIG. 3. Distance in degrees between the storm track latitude and the Hadley cell terminus latitude in the analytical solution to the EBM as a function of the meridional eddy energy flux F at the Hadley cell terminus, for 5 values of the eddy efficiency ζ' between 0.1 and 0.3. The Hadley cell terminus is assumed constant at 25°N. The dashed gray line shows the first-order approximation (10) of the storm-track distance to the Hadley cell terminus for $\zeta' = 0.2$; the dashed black line shows the second-order approximation (A16).

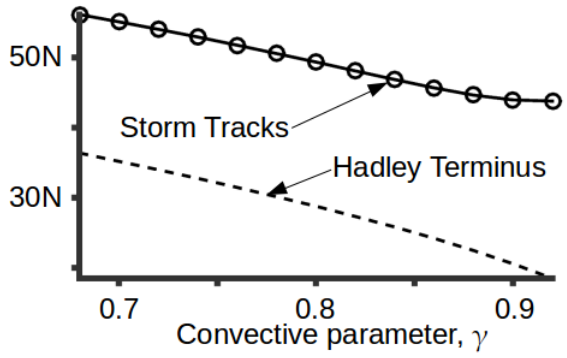

FIG. 4. Response of the full numerical solution of the EBM to changes in convective stability: Hadley cell terminus (dashed line) and storm tracks (solid line). As the convective stability decreases toward the right, the Hadley cell terminus shifts equatorward. For about $\gamma \leq 0.88$, the storm tracks shift poleward in tandem with the Hadley cell terminus; their shifts decouple for weaker convective stability ($\gamma \geq 0.88$).

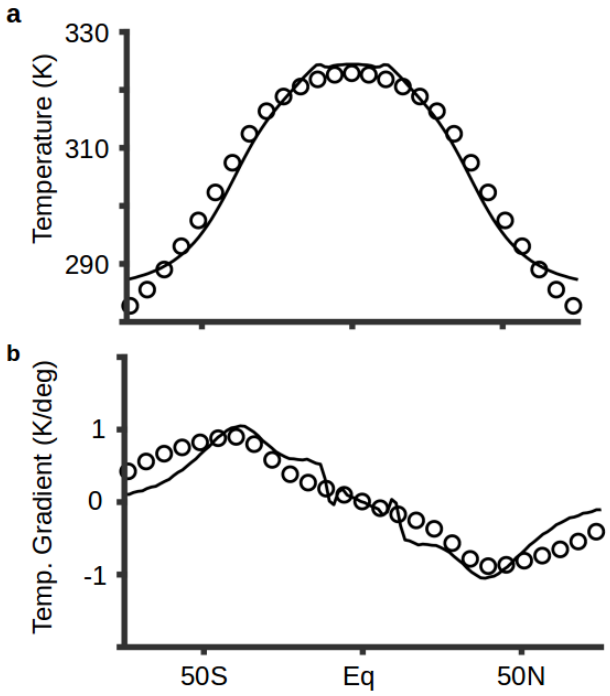

FIG. 5. Zonal-mean (a) temperature and (b) temperature gradient profiles from the GCM (solid lines) and the EBM (circles).

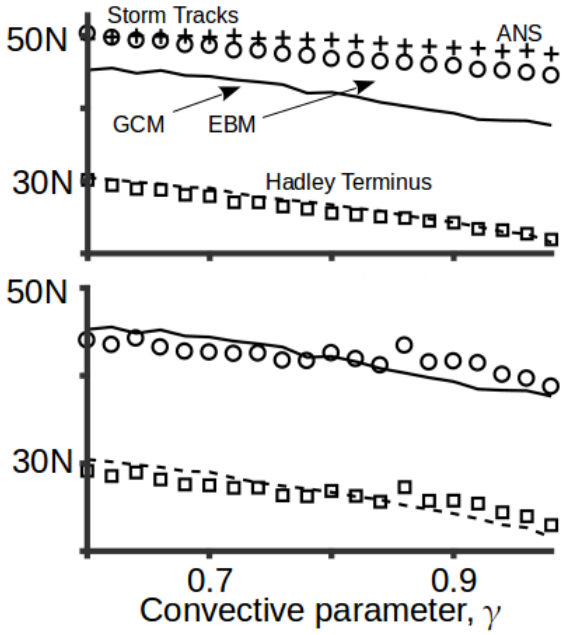

FIG. 6. (a) Storm track response to changes in deep-tropical convective stability in the idealized dry GCM (solid black line), in the full EBM with fixed tropical diffusivity (circles), and in the analytical solution of the EBM taking the Hadley cell terminus latitude in the full EBM as given (crosses). Note that deep-tropical stability is inversely proportional to the convective parameter, γ. The dashed line shows the Hadley cell terminus in the GCM and the squares show it for the EBM. (b) same as in (a), but with variable tropical diffusivity taken as the tropical average in each individual GCM simulation.

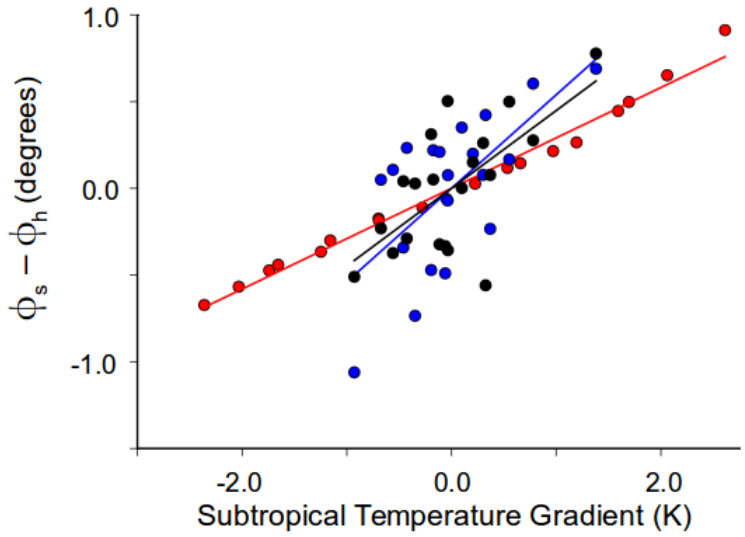

FIG. 7. Difference between the latitudes of the storm track ϕ_s and the Hadley terminus ϕ_h versus subtropical temperature gradient, for the EBM (red), the GCM (black), and the analytical EBM solution forced with parameters from the GCM but with the Hadley cell terminus assumed constant at 25°N (blue). The least-squares linear-regression lines are plotted in their respective colors. The temperature gradient has been multiplied by the Earth radius R to express it as a temperature difference in units of Kelvin. What are plotted are the anomalies relative to the arithmetic mean for each dataset.